Immunity, Volume *45*

Supplemental Information

Identification of a CD4-Binding-Site Antibody to HIV that Evolved Near-Pan Neutralization Breadth

Jinghe Huang, Byong H. Kang, Elise Ishida, Tongqing Zhou, Trevor Griesman, Zizhang Sheng, Fan Wu, Nicole A. Doria-Rose, Baoshan Zhang, Krisha McKee, Sijy O'Dell, Gwo-Yu Chuang, Aliaksandr Druz, Ivelin S. Georgiev, Chaim A. Schramm, Anqi Zheng, M. Gordon Joyce, Mangaiarkarasi Asokan, Amy Ransier, Sam Darko, Stephen A. Migueles, Robert T. Bailer, Mark K. Louder, S. Munir Alam, Robert Parks, Garnett Kelsoe, Tarra Von Holle, Barton F. Haynes, Daniel C. Douek, Vanessa Hirsch, Michael S. Seaman, Lawrence Shapiro, John R. Mascola, Peter D. Kwong, and Mark Connors

A

Clade	Virus ID	Serum ID 45	127/C	N152	N208	Z256	Z258
A	KER2018	88	160	397	471	271	494
	RWO20.2	207	956	1341	1090	754	553
	Q168.a2	251	628	509	1900	846	1170
	Q769.d22	1033	1233	1834	888	901	665
	Q769.h5	732	3032	836	472	710	431
B	JRFL.JB	18000	3750	860	1908	1444	8299
	BaL.01	1578	1308	1590	11602	2418	1369
	YU2.DG	767	320	279	1005	353	595
	PVO.04	172	496	359	170	2454	603
	TRO.11	806	940	2773	1304	1905	383
	CAAN.A2	222	93.0	1364	675	2451	338
	TRJO.58	262	749	1231	392	534	235
	THRO.18	69	189	351	2089	2057	283
	BG1168.1	79	152	167	226	264	215
	6101.1	870	267	1372	459	127	442
C	ZA012.29	301	734	39	252	112	260
	DU156.12	794	1185	2021	974	382	944
	DU422.01	97	309	325	490	296	154
	ZM106.9	298	166	256	1679	398	1164
	ZM55.28a	393	178	84.8	224	409	411
Control	SIVmac251.SG3	5	5	5	5	5	5
	Geometric Mean ID_{50}	393	504	567	769	636	546
	Median ID_{50}	300	562	673	782	622	468

C

Virus ID	Clade	IC_{50} (μg/ml) N6	F8	N17	N6 variant-1 N6H+F8K	N6 variant-2 N6H+N17K	N6 variant-3 N17H+F8K	N6 variant-4 N17H+N6K	N6 variant-5 F8H+N6K	N6 variant-6 F8H+N17K	VRC01
6540.v4.c1	AC	0.014	0.090	0.458	0.015	0.100	0.056	0.046	0.143	1.03	>50
6545.V4.C1	AC	0.430	>25	0.052	4.15	0.019	>25	>25	>25	0.113	>50
620345.c1	AE	0.338	0.545	>50	1.08	>50	0.652	1.28	1.69	6.17	>50
242-14	AG	0.256	1.50	1.16	0.269	1.57	0.255	0.307	3.78	10.9	>50
T250-4	AG	0.009	0.011	0.057	0.019	0.009	0.013	0.012	0.044	0.054	>50
HO86.8	B	0.445	0.050	>50	0.024	0.037	>25	>25	>25	0.237	>50
7165.18	B	0.709	1.38	19.2	0.764	2.13	4.61	7.20	2.90	2.02	>50
DU422.01	C	0.015	0.110	1.77	0.044	0.081	0.126	0.529	0.055	1.94	>50
DU172.17	C	0.016	0.050	0.090	0.022	0.049	0.042	0.028	0.043	0.064	>50
6322.V4.C1	C	0.027	0.095	0.387	0.056	0.073	0.118	0.153	0.143	0.194	>50
6631.V3.C10	C	0.065	0.228	0.278	0.106	0.125	0.087	0.123	0.258	0.374	>50
TZA125.17	C	0.407	0.668	3.47	0.323	1.04	0.586	0.564	1.48	1.59	>50
CAP210.E8	C	12.2	>25	>50	2.81	>50	>25	>25	>25	>50	>50
3817.v2.c59	CD	0.287	3.06	1.42	0.029	0.743	1.36	1.93	0.870	0.488	>50
57128.vrc15	D	5.74	1.84	4.34	2.38	1.93	2.79	2.15	2.71	3.28	>50
X2088.c9	G	0.048	0.128	0.186	0.018	0.181	0.091	0.037	0.162	0.293	>50
T278-50	AG	>50	>25	>50	>50	>50	>25	>25	>25	>50	>50
BL01.DG	B	>50	>25	>50	>50	>50	>25	>25	>25	>50	>50
6471.V1.C16	C	>50	>25	>50	>50	>50	>25	>25	>25	>50	>50
TV1.29	C	>50	>25	>50	>50	>50	>25	>25	>25	>50	>50
Geometric Mean IC_{50} (μg/ml)		0.163	0.247	0.621	0.146	0.173	0.233	0.269	0.395	0.644	>50
Median IC_{50} (μg/ml)		0.271	0.178	0.458	0.081	0.113	0.126	0.307	0.258	0.488	>50
Breadth (%)		80	70	65	80	70	65	65	65	75	0

B

Serum ID	VRC01-like	b12-like	HJ16-like	8ANC195-like	PG9-like	PGT128-like	2F5-like	10E8-like	3SO22-like	PGT151-like
Z258	0.40	0.21	0.22		0.15					0.03
45	0.55				0.02	0.30		0.13		
57	0.49	0.25	0.03		0.07	0.17				
127/C	0.60	0.09		0.05	0.05			0.15	0.05	
1	0.44	0.25	0.08		0.01		0.10	0.01	0.11	
CE8J	0.14	0.26				0.51		0.08		
N27		0.26				0.45		0.13	0.16	
N152				0.09		0.25		0.35	0.31	

D

```
                    1        10        20        30        40      5052A     60        70      8082ABC   90       100ABCDE      110113
                    |        |         |         |         |       | ||      |         |       |||||    |        ||||||       |  |
Heavy Chain         _________FR1_______ _CDR1____ ____FR2____ _____CDR2____ _________FR3_____________ _CDR3___ ____FR4____
IGHV1-2*02          QVQLVQSGAEVKKPGASVKVSCKASGYTFT GYYMH WVRQAPGQGLEWMG WINPNSGGTNYAQKFQG RVTMTRDTSISTAYMELSRLRSDDTAVYYCAR ---------- ----------
N6                  RAH.....TAM.......R...QT..... AHILF .F.....R....V. ..K.QY.AV.FGGG.RD ...L...VYREI...DIRG.KP.......... DRSYDDSSWALDA WGQGTTVVVSA
N17                 RAH.....TA..R.....R...ET..... AHILY .F.....R....V. ..K.QY.AV.FGGG.R. ...L...IYRD....DI.G..F.......... DRSYDDSSWALDA WGQGTTVVVSA
F8                  ........TAM.......R...QT..... AHILF .F.....R....V. ..K.QY.AV.FGGG.RD ...L...IYREI...DIRG.KL.......... DRSYGDSSWALDA WGQGTTVVASA
VRC27               Q-R.....PQ.R...S..RI..ET.....N A.IL. .F.....RSF.... ..K.KF.AV...HS... .I.L...IYRE..FLD.TG..P.......... DRLYDGSSWRLDP WGQGTRVVVSS
VRC01               ........GQM....E.MRI..R....E.I DCTLN .I.L...KRP.... .LK.RG.AV...RPL.. .......VYSD..FL..RS.TV......F.T. GKNCDYN WDPEH WGRGTPVIVSS

                    1        10        20        30        40        50        60        70        80        9096  100   107
                    |        |         |         |         |         |         |         |         |         ||    |     |
Kappa Chain         _____FR1_____ ____CDR1____ ____FR2_____ ____CDR2___ _____FR3_____________ _____CDR3____ ___FR4___
IGKV1-33*01         DIQMTQSPSSLSASVGDRVTITC QASQDISNYLN WYQQKPGKAPKLLIY DASNLET GVPSRFSGSGSGTDFTFTISSLQPEDIATYYC ----- ----------
N6                  Y.HV........V.I......N. .T..GVGSD.H ...H...R.....H HT.SV.D ..........FH.S.NL...D..AD....... QVLQF FGRGSRLHIK
N17                 Y.HV........V.A......N. .T..GVGRD.H ...H...R.....R H..SV.D .......T.FH.S.NL..ND..SD....... QVLES FGRGSRLDFK
F8                  Y.HV........V.I......N. .T..GVGSD.H ...H...R.....H H..SV.D ..........FH.S.NL..ND..AD....... QVLQF FGRGSRLHIK
VRC27               FAL.....AT.AV.......... R...G.GSD.H .....R.RP..I..H H..AR.E ......G....H.S.I...ND..LD.V..... QVLES FGQGTRLDIN
VRC01               E.VL....GT..L.P.ETAI.S. RT..-YGS-.A ....R..Q..R.V.. SG.TRAA .I.D.....RW.P.YNL...N.ESG.FGV... QQYEF FGQGTKVQVDIKR
```

E

N6 Heavy Chain

IGHV	IGHD	IGHJ	CDR3 length (amino acid)	VH mutation frequency (nt)
1-2*02	2-21*02	6*01	15	88/288 (31%)

N6 Light Chain

IGKV	IGKJ	CDR3 length (amino acid)	VK mutation frequency (nt)
1-33*01 or 1D-33*01	5*01	5	69/279 (25%)

G

mAb\gp120	K_D (M) 93TH057	DU172	X2088
N6	2.59E-09	2.81E-09	9.90E-09
VRC27	1.06E-08	NB	NB
VRC01	8.88E-09	4.98E-07	NB

H

gp120 domain	gp120 mutation	Binding affinity relative to WT (%) N6	VRC01	3BNC 117	VRC-PG04	12A21	VRC27	CD4-Ig	2G12
	WT	100	100	100	100	100	100	100	100
V2	D167N	83	77	95	42	108	37	58	100
V1V2 stem	N197T	80	72	101	39	131	28	25	100
	N262A	36	23	33	14	167	0	2	100
Loop D	D279A	15	0	0	247	188	7	49	100
	N280A	50	82	36	12	174	0	75	100
	K282A	28	33	3	12	29	57	53	100
	T283A	28	34	71	83	68	15	55	100
V3	N332A	58	72	82	31	206	57	57	3
CD4 binding loop	S365A	28	63	90	34	454	107	34	100
	G366A	27	20	27	17	6	3	7	100
	G367A	19	18	25	19	2	0	3	100
	D368A	10	1	16	12	30	0	5	100
	P369A	57	50	75	44	122	38	54	100
	E370A	30	13	31	20	16	2	5	100
	I371A	31	16	40	21	17	0	12	100
	V372A	62	33	62	15	36	15	73	100
	M373A	67	56	133	44	63	23	91	100
β23	D457A	13	22	84	0	23	19	3	100
β24	I467A	77	42	87	40	49	27	115	100
	R469A	90	49	97	6	66	0	7	100
β24-α5 connection	G471A	113	108	164	64	162	131	141	100
	G472A	51	41	56	38	97	0	2	100
	G473A	103	48	40	34	53	6	0	100
	D474A	33	21	38	0	19	0	45	100
	M475A	82	75	169	90	76	35	117	100
	R476A	65	51	171	84	73	37	79	100

F

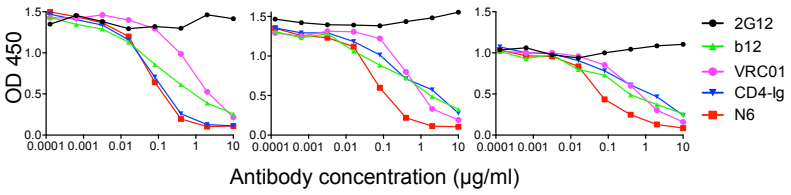

Figure S1. Donor 258 serum neutralizing profile, N6 gene sequences, neutralization activity and binding specificity, Related to Figure 1.

(A) Neutralization profile of patient sera against a 20-isolate Env-pseudovirus panel. The data show the ID_{50} of sera against each virus. ID_{50}>1000 is highlighted in red, 400<ID_{50}<1000 is in orange, and 100<ID_{50}<400 is in yellow. (B) Serum neutralization finger-print of Z258. (C) Neutralization by N6 and its variants against 20 VRC01-resistant viruses. (D) Amino acid sequences of the variable regions of N6 and its variants. Kabat numbering is used to number residues in the heavy and light chains. (E) Germline genes of N6 heavy and light chain variable regions. Germline alleles were determined using the IMGT database (http://imgt.org). (F) ELISA binding of N6 to $gp120^{YU2}$ in competition with CD4Ig-biotin, VRC01-biotin and VRC-PG04-biotin. b12, VRC01 and CD4-Ig were used as positive controls and 2G12 was used as a negative control. (G) SPR binding of N6, VRC01 and VRC27 to HIV-1 Env gp120 of 93TH075, DU172 and X2088. NB represents no binding. (H) Binding of N6 to alanine scanning mutants in the context of monomeric $gp120^{JRCSF}$ by ELISA. Amino acid numbering of mutants is based on HIV-1 HXBC2 sequence. Binding affinities to captured gp120s were measured based on the antibody concentration at half-maximal binding. 2G12 was used as a control to measure the amount of captured gp120 to standardize the effect of each mutation on antibody binding. Mutations that resulted in decreased binding of gp120 below 33% relative to that of wild type are highlighted in yellow.

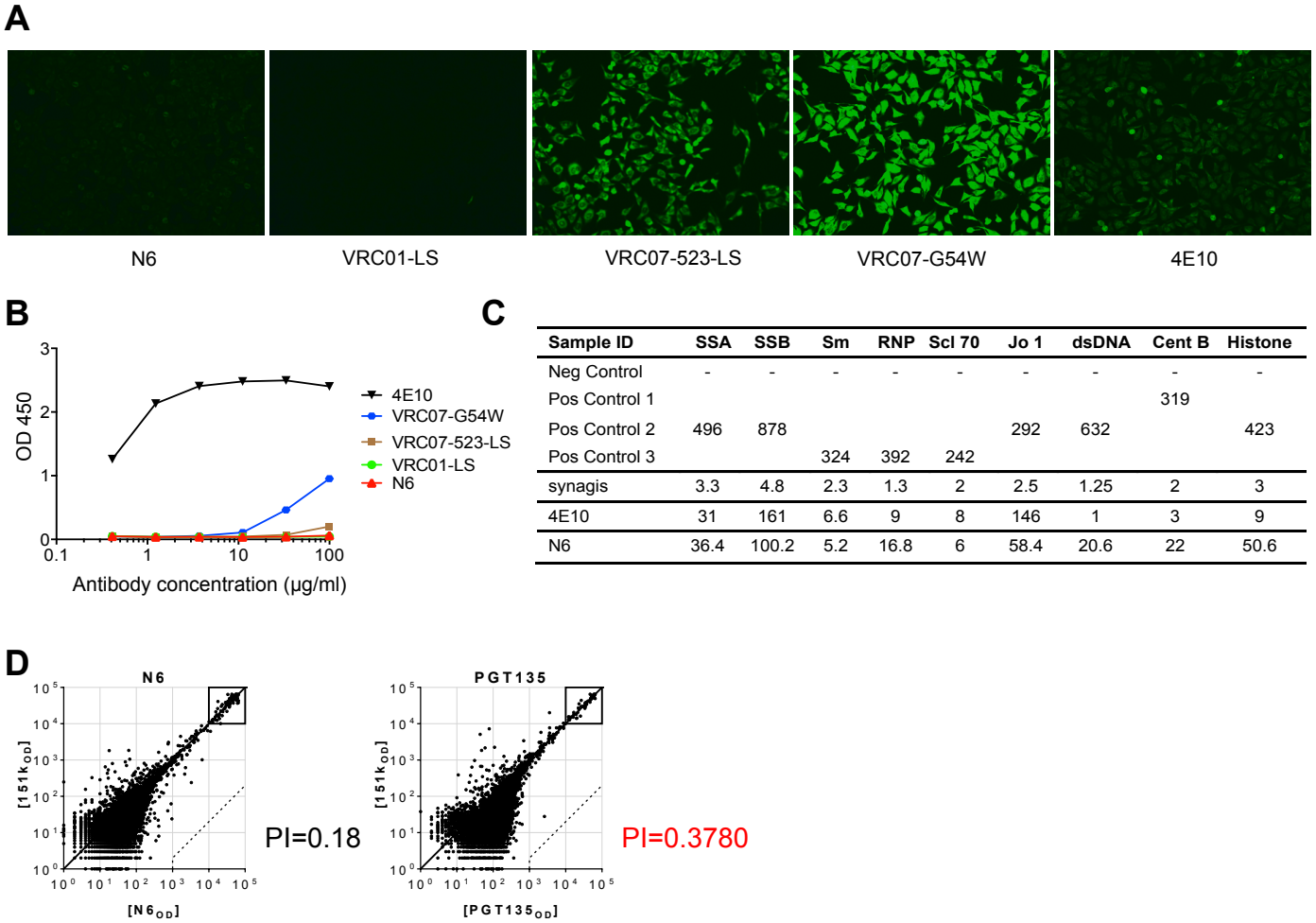

Sample ID	SSA	SSB	Sm	RNP	Scl 70	Jo 1	dsDNA	Cent B	Histone
Neg Control	-	-	-	-	-	-	-	-	-
Pos Control 1								319	
Pos Control 2	496	878				292	632		423
Pos Control 3			324	392	242				
synagis	3.3	4.8	2.3	1.3	2	2.5	1.25	2	3
4E10	31	161	6.6	9	8	146	1	3	9
N6	36.4	100.2	5.2	16.8	6	58.4	20.6	22	50.6

Figure S2. Autoreactivity of N6, Related to Figure 1.

(A) Reactivity of N6 with HEP-2 epithelial cells. VRC07-523-LS, VRC07-G54W and 4E10 were used as positive controls. VRC01-LS was used as a negative control. Antibody concentration was 25 µg/ml. All pictures are shown at 400X magnification. (B) ELISA binding of N6 to cardiolipin. Controls are as above. (C) Reactivity of N6 with autoantigens as detected by Luminex assay. 4E10 was used as a positive control. The cut off for positive is 120 luminex units. Therefore, N6 is considered negative. Synagis, an anti-RSV monoclonal antibody, was used as a negative control. SSA, Sjogren's syndrome antigen A; SSB, Sjogren syndrome antigen B; Sm, Smith antigen; RNP, ribonucleoprotein; Scl 70, scleroderma 70; Jo1, antigen; CentrB, centromere B. (D) N6 and PGT135 bNAbs binding in protein microarrays. Representative examples of InVitrogen ProtoArrays™ blotted with N6 (left), PGT135 (right) or 151K control Ab. Axis values are MFI in the 151K array (y axis) or test Ab array (x axis); each dot represents the average MFI of duplicate array proteins. The diagonal line indicates equal binding by the test Ab and 151K. Internal controls for loading of Ab and secondary detection reagent were equally bound by Ab pairs (boxes). Dashed lines indicate the 500-fold test/control ratio that defines significant autoreactivity and polyreactivity indices (PI) > 0.21 are considered polyreactive. N6 is neither auto- or polyreactive while PGT135 is polyreactive (Liu et al. J Virol. 89:784;2015).

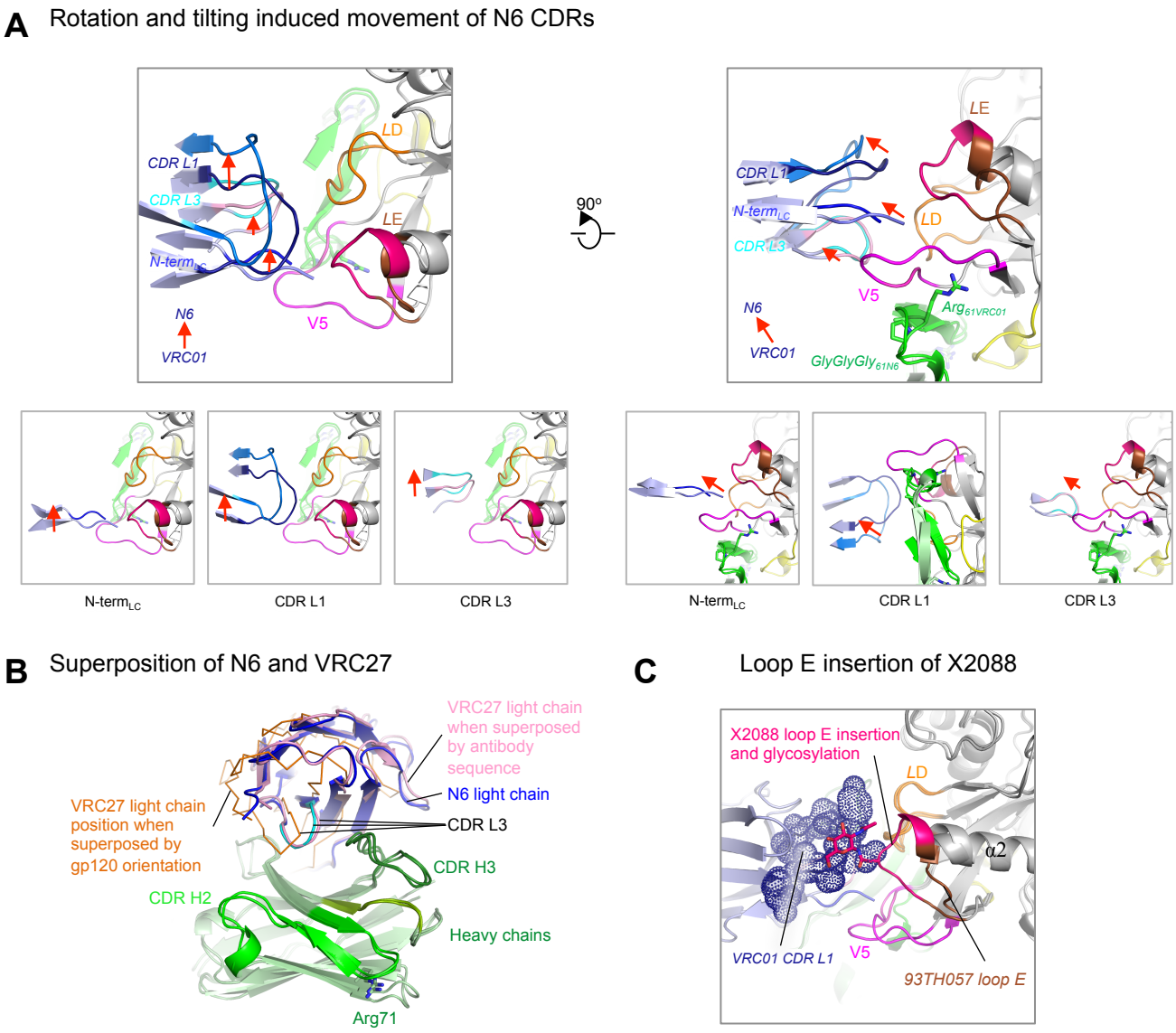

Figure S3. Specific features of N6 recognition of HIV-1 gp120, Related to Figure 3.
(A) Unusual rotation and tilting of N6 comparing to other VRC01-class antibodies led to the positional shift of its structural components. These shifts resolved potential steric hindrance caused by mutations and inserts in HIV-1 gp120 that would otherwise confer resistance to N6. N-termini, CDR L1 and CDR L3 of light chains of VRC01 and N6 are shown to demonstrate the positional shifts in two views 90° apart. Panels below each view show comparison of each individual component with the other two omitted for clarity. Structure of X2088 is displayed in a cartoon with the loop E insertion colored hot pink. (B) Superposition of the variable domains of N6 and VRC27 by different alignment methods. VRC27 variable domain superposed onto the N6 structure by aligning antibody sequences are shown in cartoon and colored pink for its light chain. The position of VRC27 light chain when superposed by N6- and VRC27-bound gp120 is shown in orange ribbon. It is evident that the positional difference of N6 from VRC27 (and other VRC01 antibodies) was not due to specially evolved heavy chain and light chain interfaces. Rather, the relative rotation of N6 light chain was the result of special recognition mode of N6 to HIV-1 gp120. Heavy chains were colored in shades of green with Arg71 shown in sticks. Light chain of N6 was shown in blue with CDR L3 colored cyan. (C) The insertion of X2088 loop E added one helix to the end of the α2 helix and a glycosylation site. The longer loop and added glycan are positioned to clash with the CDR L1 of most VRC01-class antibodies except N6. VRC01 is modeled in its gp120-bound position to show the CDRL1 clash with the loop E insertion and glycan. Normal loop E of 93TH057 gp120 in the VRC01 complex is show for comparison.

A

	Virus ID	IC_{50} (μg/ml) N6	IC_{50} (μg/ml) VRC01	Env sequence Loop D (275-283)	Env sequence CD4 BLP (362-374)	Env sequence V5 (458-469)
Reference Viruses	HXBC2	0.005	0.040	VNFTDNAKT	KQSSGGDPEIVTH	GGNSNNESE IFR
	JRCSF	0.066	0.160	DNFTDNAKT	THSSGGDPEIVMH	GGKNESEIE IFR
	93TH057	0.095	1.32	ENLTNNAKT	QPPSGGDLEITMH	GGANNTSNE TFR
N6-Sensitive Viruses	6540.v4.c1	0.014	>50	EHIGNSAKN	KNSSGGDIEITTH	YGNNNSDNE IFR
	6545.V4.C1	0.430	>50	EHIENNAKN	KNSSGGDIEITTH	YGNSSSDNE TFR
	620345.c1	0.338	>50	EDITKNTKT	QPPSGGDLEVTTH	GDGGPTADNE TFR
	242-14	0.256	>50	ENISNNGKT	TNHSGGDLEVTTH	GPNSTQNE TFR
	T250-4	0.009	>50	ENTIDNAKT	EKHSGGDLEVITH	GGENRTDNGTE IFR
	HO86.8	0.445	>50	ENFTKNEKT	NQSTGGDPETAMF	GDKNNKSTE VFR
	7165.18	0.709	>50	ENFTDNVKT	MQHSGGDPEIVTH	GGENRTDGTE IFR
	DU422.01	0.015	>50	ENLTNNIKT	EPSSGGDLEVTTH	GGENSTEG VFR
	DU172.17	0.016	>50	ENLTNNAKI	APSSGGDLEITTH	GGKEKNDTE TFR
	6322.V4.C1	0.027	>50	ENLTNNAKI	QPHSGGDLEVVTH	GGKDNNMTE IFR
	6631.V3.C10	0.065	>50	ENLTNNAKI	ESHSGGDLEITTH	GGPNSTNE TFR
	TZA125.17	0.407	>50	ENLTNNAKT	KPAVVGGDLEITTH	GGNNTNGTE TFR
	CAP210.E8	12.2	>50	ENISNNVKT	APPVGGDLEITTH	GGENKTENNDTEIFR
	3817.v2.c59	0.287	>50	ENVTNNAKT	SPSSGGDPEITTH	GGLNTSNNE TFR
	57128.vrc15	5.74	>50	ENLTNNAKI	NASSGGDPEITTH	GGGADNNRQNE TFR
	X2088.c9	0.048	>50	ENLTNNAKV	NSPAGGDLEITTH	GVNDTHDKENE TFR
N6-Resistant Viruses	T278-50	>50	>50	KNISANAKT	TKPSGGDLEITTH	GEGDEKANE TFR
	BL01.DG	>50	>50	KNFTQNAET	NPPIRGGDPEIVMH	GGKNGTEGTE IFR
	6471.V1.C16	>50	>50	KDLNNTGNT	SPHPGGDLEVTMH	GDKTSNDPDTD VFR
	TV1.29	>50	>50	ENLTENTKT	KPHAGGDIEITMH	GGFNTTNNTE TFR
Patient Autologous Viruses	Z258.2012.SGA1,2,3,5	>50	>50	DNFSRNTKN	QPHSGGDPEVVRH	GGNNPEGKNNTEIFR
	Z258.2014.SGA1,4,6,9,11	>50	>50	DNFSRDTKN	QPHSGGDPEVVRH	GGNKNTTKE IFR
	Z258.2014.SGA3,7	>50	>50	DNFSDNNKN	DAHSGGDPEVVMH	GGNNIGGENNTEIFR

B

Virus	Env sequence Loop D (275-283)	Env sequence CD4 BLP (362-374)	Env sequence V5 (458-469)	IC_{50} (μg/ml) N6	VRC01	3BNC 117	VRC-PG04	VRC27	12A21	CD4-Ig	2G12
HXBC2	VNFTDNAKT	KQSSGGDPEIVTH	GGNSNNESE IFR	0.162	0.827	1.89	1.25	1.59	2.64	0.299	0.393
JRCSF	DNFTDNAKT	THSSGGDPEIVMH	GGKNESEIE IFR	0.083	0.782	1.15	1.08	0.415	1.10	0.103	0.325
93TH057	ENLTNNAKT	QPPSGGDLEITMH	GGANNTSNE TFR	0.022	0.599	0.305	0.575	1.21	0.086	0.084	>5
T278-50	KNISANAKT	TKPSGGDLEITTH	GEGDEKANE TFR	>5	>5	>5	>5	>5	2.59	1.41	1.72
T278-50.V5 Swap	KNISANAKT	TKPSGGDLEITTH	GGNSNNESE TFR	>5	>5	>5	>5	>5	2.59	0.908	2.01
T278-50.Loop D mut (A279D)	KNISDNAKT	TKPSGGDLEITTH	GEGDEKANE TFR	0.719	>5	>5	>5	>5	2.52	0.115	1.62
T278-50.Loop D mut/V5 Swap	KNISDNAKT	TKPSGGDLEITTH	GGNSNNESE TFR	0.324	1.59	1.84	1.82	>5	2.53	0.118	1.23
TV1.29	ENLTENTKT	KPHAGGDIEITMH	GGFNTTNNTE TFR	>5	>5	>5	>5	>5	2.47	>5	>5
TV1.29.V5 Swap	ENLTENTKT	KPHAGGDIEITMH	GGKNESEI E TFR	>5	>5	>5	>5	>5	>5	>5	>5
TV1.29 T281A	ENLTENAKT	KPHAGGDIEITMH	GGFNTTNNTE TFR	>5	>5	>5	>5	>5	2.57	2.36	>5
TV1.29 E279D	ENLTDNTKT	KPHAGGDIEITMH	GGFNTTNNTE TFR	>5	>5	>5	>5	>5	2.57	2.52	>5
TV1.29.Loop D mut (E279D T281A)	ENLTDNAKT	KPHAGGDIEITMH	GGFNTTNNTE TFR	0.922	>5	>5	>5	>5	2.57	>5	>5
TV1.29.Loop D mut/V5 Swap	ENLTDNAKT	KPHAGGDIEITMH	GGKNESEI E TFR	0.453	1.52	1.83	1.67	2.10	2.31	1.08	1.22
TV1.29.Loop D mut/CD4 BLP mut/V5 Swap	ENLTDNAKT	KQSSGGDIEITMH	GGKNESEI E TFR	0.911	2.21	1.53	1.38	2.59	2.51	1.76	1.43
BL01.DG	KNFTQNAET	NPPIRGGDPEIVMH	GGKNGTEGTE IFR	>5	>5	>5	>5	>5	2.54	0.109	0.654
BL01.V5 Swap	KNFTQNAET	NPPIRGGDPEIVMH	GGKNESEIE IFR	>5	>5	>5	>5	>5	2.55	0.055	0.516
BL01 E282K	KNFTQNAKT	NPPIRGGDPEIVMH	GGKNGTEGTE IFR	>5	>5	>5	>5	>5	2.58	2.56	>5
BL01 Q279N	KNFTNNAET	NPPIRGGDPEIVMH	GGKNGTEGTE IFR	>5	>5	>5	>5	>5	2.56	2.49	>5
BL01.Loop D mut (Q279D E282K)	KNFTDNAKT	NPPIRGGDPEIVMH	GGKNGTEGTE IFR	1.06	>5	>5	>5	>5	2.59	0.153	0.462
BL01.Loop D mut/V5 Swap	KNFTDNAKT	NPPIRGGDPEIVMH	GGKNESEIE IFR	0.726	4.98	>5	>5	>5	2.56	0.081	0.643
BL01.Loop D/CD4 BLP mut/V5 Swap	KNFTDNAKT	KQSSGGDPEIVMH	GGKNESEIE IFR	0.173	1.39	>5	1.91	>5	2.00	0.080	0.293
Z258 2012 SGA5	DNFSRNTKN	QPHSGGDPEVVRH	GGNNPEGKNNTEIFR	>5	>5	>5	>5	>5	2.55	0.142	>5
Z258 2012 SGA5 V5 swap	DNFSRNTKN	QPHSGGDPEVVRH	GGKNESEIE IFR	>5	>5	>5	>5	>5	2.01	1.35	>5
Z258 2012 SGA5 CD4 BLP mut	DNFSRNTKN	THSSGGDPEIVMH	GGNNPEGKNNTEIFR	>5	>5	>5	>5	>5	2.34	0.597	>5
Z258.2012.SGA5 T281A	DNFSRNAKN	QPHSGGDPEVVRH	GGNNPEGKNNTEIFR	>5	>5	>5	>5	>5	2.02	1.51	>5
Z258.2012.SGA5 N283T	DNFSRNTKT	QPHSGGDPEVVRH	GGNNPEGKNNTEIFR	>5	>5	>5	>5	>5	2.15	1.05	>5
Z258.2012.SGA5 R279D	DNFSDNTKN	QPHSGGDPEVVRH	GGNNPEGKNNTEIFR	0.331	1.16	0.700	>5	>5	2.32	0.857	>5
Z258 2012 SGA5 Loop D mut (R279D T281A N283T)	DNFSDNAKT	QPHSGGDPEVVRH	GGNNPEGKNNTEIFR	0.062	0.779	0.512	0.835	2.18	2.64	0.086	>5
Z258 2012 SGA5 Loop D mut/ V5 swap	DNFSDNAKT	QPHSGGDPEVVRH	GGKNESEIE IFR	0.165	1.84	1.04	1.54	>5	2.47	0.184	>5
Z258 2012 SGA5 Loop D/ CD4 BLP mut/ V5 swap	DNFSDNAKT	THSSGGDPEIVMH	GGKNESEIE IFR	0.468	1.43	0.098	0.952	>5	2.11	0.932	>5

C

Virus	Env sequence Loop D (275-283)	Env sequence CD4 BLP (362-374)	Env sequence V5 (458-469)	IC_{50} (μg/ml) N6	VRC01	3BNC 117	VRC-PG04	VRC27	12A21	CD4-Ig	2G12	Fold change relative to WT N6	VRC01	3BNC 117	VRC-PG04	VRC27	12A21	CD4-Ig	2G12
JRCSF	DNFTDNAKT	THSSGGDPEIVMH	GGKNESEIE IFR	0.066	0.160	0.041	0.186	0.290	0.186	2.84	0.220	1	1	1	1	1	1	1	1
Z258.2012.SGA5	DNFSRNTKN	QPHSGGDPEVVRH	GGNNPEGKNNTEIFR	>50	>50	>50	>50	>50	>50	0.179	>50	>757.5	>312.5	>1219.5	>269.3	>172.5	>269.3	>17.6	>227.7
JRCSF-Z258 Loop D Swap	DNFSRNTKN	THSSGGDPEIVMH	GGKNESEIE IFR	0.730	>50	0.789	>50	>50	>50	17.9	12.8	11.1	312.5	19.2	269.3	172.5	269.3	6.3	58.3
JRCSF-Z258 CD4BLP Swap	DNFTDNAKT	QPHSGGDPEVVRH	GGKNESEIE IFR	0.202	0.483	0.063	0.359	30.7	0.327	3.69	0.231	3.1	3.0	1.5	1.9	105.9	1.8	1.3	1.1
JRCSF-Z258 V5 Swap	DNFTDNAKT	THSSGGDPEIVMH	GGNNPEGKNNTEIFR	0.114	0.166	0.019	0.039	0.074	0.046	4.05	0.637	1.7	1.0	0.5	0.2	0.3	0.2	1.4	2.9

Figure S4. N6 epitope, Related to Figure 4

(A) Amino acid sequences of loop D, CD4 BLP and V5 region of N6-sensitive, resistant, and the patient Z258 autologous viruses. HXBC2, JRCSF and 93TH057 are listed at the top as references. Sequence numbering is base on HXBC2. (B) ELISA binding of N6 to N6-resistant viruses and their reverse mutants. EC50 values < 0.1 μg/ml are colored red, values between 0.1-1 μg/ml are colored orange, values > 1 μg/ml are colored yellow. Sequence variation of gp120 displayed by N6-resistant viruses and Z258 autologous viruses compared to reference sequences are listed in bold red. Reverse mutations were highlighted in bold and underlined. (C) N6 neutralization sensitivity of JRCSF with Z258 autologous virus mutations. Autologous virus Z258.2012.SGA5 was selected and the sequence of its loop D, CD4 BLP or V5 region was substituted into the JRCSF Env sequence. Z258 autologous virus variations from the JRCSF sequences are labeled in red. Neutralization fold change was calculated by IC_{50} of JRCSF mutant/ IC_{50} of JRCSF WT. Values >5 are highlighted in yellow.

Antibody	IC_{50} (μg/ml)								Median IC_{50} (μg/ml)	Fold change	Breadth
	VRC01-Resistant Viruses						VRC01-Sensitive Viruses				
	6540.v4.c1	T250-4	HO86.8	6631.V3.C10	DU422.01	X2088.c9	BG1168.01	CAAN.A2			
N6	0.011	0.014	0.445	0.065	0.020	0.015	0.031	0.086	0.018		
VRC01	>50	>50	>50	>50	>50	>50	0.576	1.06	50.00		
VRC01 $G54Y_{N6\ HC}$	>50	>50	>50	>50	>50	>50	0.056	1.31	50.00	1	0
VRC01 $ARP60\text{-}62GGG_{N6\ HC}$	>50	>50	>50	>50	>50	>50	1.53	3.23	50.00	1	0
VRC01 N6CDRH3	>50	>50	>50	>50	>50	>50	>50	2.23	50.00	1	0
VRC07 N6CDRH3	>50	>50	>50	>50	>50	>50	>50	2.18	50.00	1	0
VRC27 N6 FRH1	1.36	18.9	>50	>50	>50	29.8	0.118	0.264	44.90	2566	50
VRC27 N6 CDRH1	5.38	>50	>50	>50	>50	>50	0.802	0.440	50.00	2857	17
VRC27 N6 FRH2	5.01	>50	>50	>50	>50	>50	0.112	0.399	50.00	2857	17
VRC27 N6 CDRH2	0.782	0.722	>50	>50	>50	>50	0.146	0.477	50.00	2857	33
VRC27 N6 FRH3	1.32	19.7	>50	>50	>50	>50	0.113	0.302	50.00	2857	33
VRC27 N6 CDRH3	3.74	>50	>50	>50	>50	>50	0.207	0.443	50.00	2857	17
N6 $Y54G_{VRC01\ HC}$	0.019	0.045	>50	0.396	5.68	0.728	0.122	0.146	0.562	32	83
N6 $GGG60\text{-}62ARP_{VRC01\ HC}$	0.049	0.061	>50	0.854	0.346	0.150	0.146	0.906	0.248	14	83
N6 VRC01FRH1	0.631	0.021	0.100	0.263	32.0	0.108	0.093	0.571	0.19	11	83
N6 VRC01CDRH1	>50	>50	>50	>50	>50	2.08	0.111	0.394	50.00	2857	17
N6 VRC01FRH2	0.009	0.003	0.061	0.042	0.056	0.033	0.024	0.133	0.037	2	100
N6 VRC01CDRH2	>50	>50	>50	>50	>50	>50	0.076	0.125	50.00	2857	0
N6 VRC01FRH3	4.82	0.017	2.14	0.152	>50	0.107	0.120	0.309	1.146	65	83
N6 VRC01CDRH3	>50	4.52	>50	0.565	6.13	0.191	0.116	0.484	5.33	304	67
N6 VRC01FRL1	0.425	0.166	16.8	0.642	4.79	1.14	0.134	1.01	0.89	51	100
N6 VRC01CDRL1	0.070	0.007	>50	>50	>50	>50	0.045	0.061	50.00	2857	33
N6 VRC01FRL2	0.008	0.011	0.002	0.168	0.069	0.070	0.067	0.223	0.040	2	100
N6 VRC01CDRL2	0.043	0.006	0.024	0.035	0.030	0.034	0.057	0.163	0.032	2	100
N6 VRC01FRL3	0.003	0.008	>50	>50	>50	>50	0.036	0.098	50.00	2857	33
N6 VRC01CDRL3	0.356	0.045	>50	0.139	0.110	0.125	0.189	0.442	0.132	8	83
N6 $QY53\text{-}54KF_{VRC27\ HC}$	0.018	0.011	0.092	0.072	0.044	0.067	3.14	0.178	0.056	2	100
N6 $F59Y_{VRC27\ HC}$	0.014	0.010	4.86	0.087	0.0010	0.055	0.127	0.280	0.034	2	100
N6 $GGG60\text{-}62AHS_{VRC27\ HC}$	0.823	0.023	>50	0.089	0.467	0.078	0.017	0.118	0.278	16	83
N6 $RD64\text{-}65QG_{VRC27\ HC}$	8.24	0.051	>50	0.191	3.60	0.043	0.112	0.363	1.893	108	83
N6 VRC27FRH1	0.056	0.079	>50	0.561	10.5	0.184	0.193	0.896	0.373	21	83
N6 VRC27CDRH1	0.229	0.023	>50	0.122	0.759	0.070	0.085	0.244	0.176	10	83
N6 VRC27FRH2	0.03	0.041	5.21	0.262	0.246	0.143	0.160	0.437	0.195	11	100
N6 VRC27CDRH2	0.121	1.57	>50	1.17	4.74	0.171	0.089	0.392	1.370	78	83
N6 VRC27FRH3	0.043	0.048	>50	0.540	2.38	0.509	0.174	0.519	0.525	30	83
N6 VRC27CDRH3	0.068	0.015	>50	0.266	0.842	0.068	0.049	0.154	0.167	10	83
N6 VRC27FRL1	0.007	0.017	0.173	0.045	0.011	0.031	0.110	0.271	0.024	1	100
N6 VRC27CDRL1	0.075	0.012	0.194	0.100	0.007	0.061	0.092	0.219	0.068	4	100
N6 VRC27FRL2	0.060	0.010	0.790	0.081	0.019	0.056	0.059	0.182	0.058	3	100
N6 VRC27CDRL2	0.071	0.012	0.073	0.084	0.014	0.054	0.046	0.096	0.062	4	100
N6 VRC27FRL3	0.019	0.009	>50	0.059	0.039	0.041	0.095	0.122	0.040	2	83
N6 VRC27CDRL3	0.178	0.013	0.021	0.077	0.087	0.102	0.021	0.180	0.082	5	100

Figure S5. Contributions of N6 paratope components to its breadth and potency, Related to Figure 5.
Neutralization of antibody mutants with substitutions of key contact residues, CDR or framework from N6, VCR01 or VRC27. IC_{50} values <0.1μg/ml are highlighted in red, values between 0.1-1μg/ml are highlighted in orange, values between 1-10 μg/ml are highlighted in yellow, and values between 10-50 μg/ml are highlighted in green. Median IC_{50} is calculated based on all VRC01-resistant viruses. For those IC_{50}>50, a value of 50 was assigned.

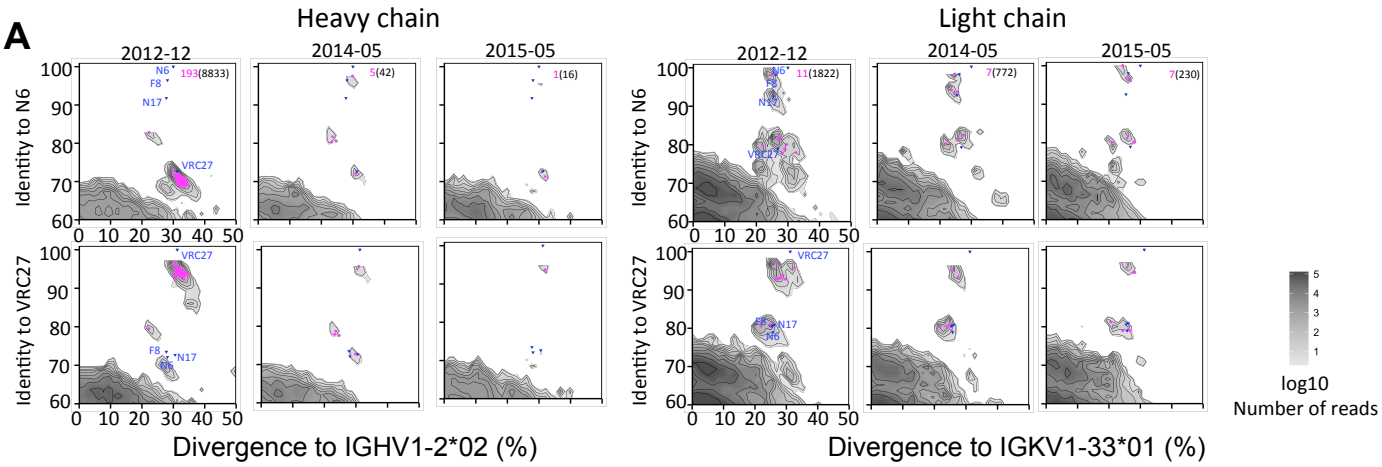

B

```
                  1        10        20        30        40        5052A     60        70        8082ABC   90        100ABCDE  110113
                  |        |         |         |         |         | ||      |         |         | ||||    |         ||||||    |   |
Heavy Chain       _____________FR1_____________ _CDR1 _____FR2_____ _______CDR2_______ _____________FR3_____________ ____CDR3_____ ____FR4____
N6 paratope                               *   * *       *   * * ********** *     * **                    *** *
IGHV1-2*02        QVQLVQSGAEVKKPGASVKVSCKASGYTFT GYYMH WVRQAPGQGLEWMG WINPNSGGTNYAQKFQG RVTMTRDTSISTAYMELSRLRSDDTAVYYCAR ------------ -----------
      I1          RGH.....T.........R...ET...... A.IL. .F.....R...... ..K.KY.AV...HA... ...L...IYRD....D..G..F........AR DRVYDDSSWQLDP WGQGTSVIVSS
      I2          RGH.....T.........R...ET...... AHIL. .F.....R...... ..K.KY.AV...HA... ...L...IYRD....D..G..F........AR DRVYDDSSWQLDP WGQGTSVIVSS
      I3          RAH.....TA........R...ET...... AHILY .F.....R....V. ..K.QY.AV.FGGG.R. ...L...IYRD....DI.G..F........AR DRSYDDSSWALDA WGQGTTVVVSA
      I4          RAH.....TAM.......R...QT...... AHILF .F.....R....V. ..K.QY.AV.FGGG.RD ...L...IYREI...DIRG.KL.......AR DRSYGDSSWALDA WGQGTTVVVSA
      N6          RAH.....TAM.......R...QT...... AHILF .F.....R....V. ..K.QY.AV.FGGG.RD ...L...VYREI...DIRG.KP.......AR DRSYGDSSWALDA WGQGTTVVVSA
      I5          SQR.....PQ.....S..RI..ET...... A.IL. .F.....RS..... ..K.KF.AV...HS... .I.L...IYRE..FLD.TG..F........AR DRLYDGSSWRLDP WGQGTRVIVSS
     VRC27        Q-R.....PQ.R...S..RI..ET.....N A.IL. .F.....RSF.... ..K.KF.AV...HS... .I.L...IYRE..FLD.TG..F........AR DRLYDGSSWRLDP WGQGTRVVVSS

                  1        10        20        30        40        50        60        70        80        9096 100   107
                  |        |         |         |         |         |         |         |         |         || |   |     |
Kappa Chain       _____________FR1_____________ ____CDR1____ _____FR2_____ _CDR2__ _____________FR3_____________ _CDR3 ___FR4____
N6 paratope       ***                         **** *                                                          ****
IGKV1-33*01       DIQMTQSPSSLSASVGDRVTITC QASQDISNYLN WYQQKPGKAPKLLIY DASNLET GVPSRFSGSGSGTDFTFTISSLQPEDIATYYC ----- ----------
      I1          Y..V........V.......... ....GVG.D.H .......R....... ...T..A ..........FH.S.....NG...D....... QVLES FGQGTRLEIK
      I2          Y.HV........V.......... ....GVG.D.H .......R....... ...T..E ........T.FH.S.....NG...D....... QVLES FGQGTRLEIK
      I3          Y.HV........V.......... ....GVGSD.H .......R......H H..T..E ........T.FH.S.....ND...D....... QVLES FGQGTRLEIK
      I4          Y.HV........V........N. .T..GVGSD.H ...H...R......H H..SV.D ........T.FH.S.NL..ND..AD....... QVLES FGRGSRLDIK
      I5          Y.HV........V.I......N. .T..GVGSD.H ...H...R......H H..SV.D ........T.FH.S.NL..ND..AD....... QVLQS FGRGSRLDIK
      I6          Y.HV........V.I......N. .T..GVGSD.H ...H...R......H H..SV.D ..........FH.S.NL..ND..AD....... QVLQF FGRGSRLHIK
      N6          Y.HV........V.I......N. .T..GVGSD.H ...H...R......H HT.SV.D ..........FH.S.NL...D..AD....... QVLQF FGRGSRLHIK
      I7          Y.HV.......AV.......... ....GVGSD.H .....R.RP..I..H H..AR.E ..........FH.S.....ND...D....... QVLES FGQGTRLEIK
      I8          Y.HV.......AV.......... ....GVGSD.H .....R.RP..I..H H..AR.E ..........FH.S.....ND...D.F..... QVLES FGQGTRLEIK
      I9          Y.HV.......AV.......... R...GVGSD.H .....R.RP..I..H H..AR.E ..........FH.S.....ND...D.F..... QVLES FGQGTRLEIK
     I10          Y.HV.......AV.......... R...G.GSD.H .....R.RP..I..H H..AR.E ..........FH.S.....ND...D.V..... QVLES FGQGTRLDIK
     VRC27        ...........AV.......... R...G.GSD.H .....R.RP..I..H H..AR.E ......G....H.S.I...ND..LD.V..... QVLES FGQGTRLDIK
```

Figure S6. Development of N6 within the VRC27-lineage in donor Z258, Related to Figure 6.
(A) Heavy and light chains Identity–divergency plots from donor Z258 samples in 2012, 2014 and 2015. Sequences are plotted as a function of sequence identity to the N6 (top row) and VRC27 (bottom row) and of sequence divergence from heavy chain IGHV1-2*02 (left) or light chain IGKV1-33*01(right) germline V genes. Shading indicates the number of sequences. The identified members of VRC27 lineage were ploted with pink dots. (B) Amino acid sequences of variable region of NGS inferred intermediates compared to N6. Residues in red represent substitutions from the I1 sequences of heavy and light chains. Kabat numbering is used for numbering residues in the heavy and light chains.

Table S2. Crystallographic Data Collection and Refinement Statistics. Related to Figure 2.

Complex (antibody-gp120)	N6-93TH057	N6-DU172	N6-X2088
PDB ID	5TE6	5TE7	5TE4
Data collection			
Space group	P 2_1 2_1 2_1	P 2_1 2_1 2_1	P 2_1 2_1 2_1
Cell dimensions			
a, *b*, *c* (Å)	64.7, 65.8, 238.0	62.7, 65.5, 241.5	64.8, 72.2, 218.1
α, β, γ (°)	90.0, 90.0, 90.0	90.0, 90.0, 90.0	90.0, 90.0, 90.0
Resolution (Å)	50.0-2.40 (2.44-2.40)*	50.0-2.15 (2.19-2.15)	50.0-2.75 (2.80-2.75)
R_{sym} or R_{merge}	0.12 (0.65)	0.079 (0.56)	0.095 (0.85)
R_{pim}	0.06	0.05	0.04
CC(1/2)	0.92 (0.71)	0.91 (0.71)	0.87 (0.14)
$I/\sigma I$	16.5 (1.6)	28.3 (2.2)	21.7 (1.4)
Completeness (%)	97.0 (84.3)	96.2 (90.2)	87.5 (50.9)
Redundancy	4.6 (3.6)	4.2 (3.1)	5.4 (2.1)
Refinement			
Resolution (Å)	43.8- 2.40 (2.44 - 2.40)	44.52 - 2.15 (2.23 - 2.15)	40.18 - 2.66 (2.76 -2.66)
No. reflections	38787	52793	25542
R_{work}/ R_{free}	0.232/0.282	0.190/0.228	0.219/0.275
No. atoms			
Protein	5987	5976	6024
Ligand/ion	169	170	222
Water	91	315	25
Wilson B (Å^2)	50.7	44.1	75.9
B-factors (Å^2)			
Protein	72.6	57.8	97.1
Ligand/ion	62.3	91.9	145.1
Water	51.7	50.9	71.1
R.m.s deviations			
Bond lengths (Å)	0.003	0.003	0.002
Bond angles (º)	0.54	0.54	0.53
Ramachandran statistics			
Favored (%)	96.0	97.3	96.0
Outliers (%)	0.3	0.3	0.1

*Values in parenthesis denote highest resolution shell.

Table S3, related to Figure 2. Contribution of antibody structural components to recognition of HIV-1 gp120.

	Heavy chain contact area (Å^2)*			Light chain contact area (Å^2)		
	N6	**VRC01**	**VRC27**	**N6**	**VRC01**	**VRC27**
FRW 1				135.2	36.9	65.5
CDR 1	28.7	18.0	23.6	110.5	125.4	88.5
FRW 2	20.9	26.5	29.9			
CDR 2	626.6	592.2	612.6			
FRW 3	117.7	108.9	124.8			
CDR 3	152.0	121.5	156.9	140.0	187.8	145.0
Total	945.9	867.1	947.8	385.7	350.1	299.0

*Interface between gp120 and antibody were analyzed with the PISA server (http://www.ebi.ac.uk/pdbe/prot_int/pistart.html) (Krissinel and Henrick, 2007).

Table S5, related to Figure 4. Amino acid sequences of Z258 autologous virus Env,.

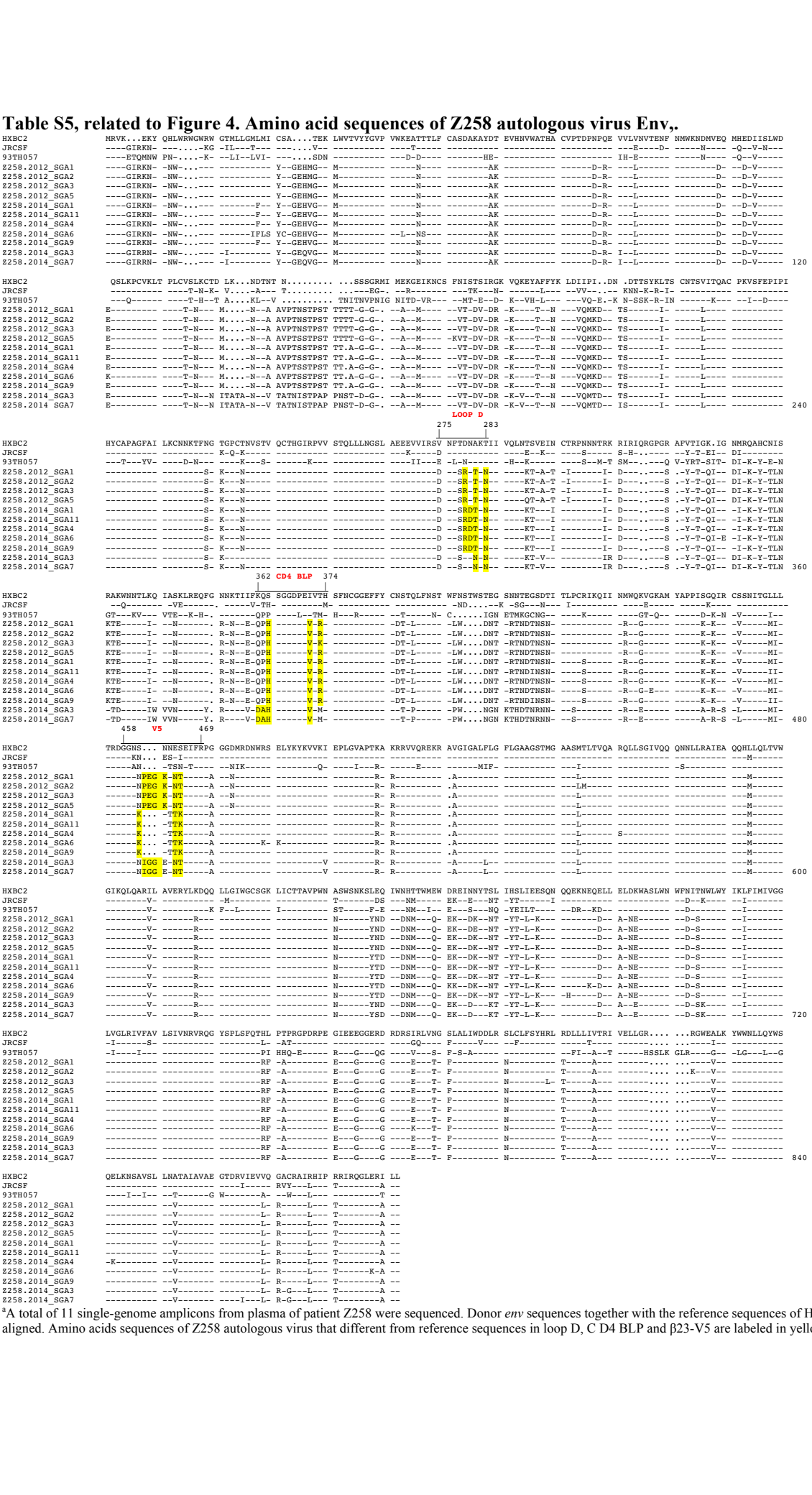

[a]A total of 11 single-genome amplicons from plasma of patient Z258 were sequenced. Donor *env* sequences together with the reference sequences of HXB2, JRCSF and 93TH057 are aligned. Amino acids sequences of Z258 autologous virus that different from reference sequences in loop D, C D4 BLP and β23-V5 are labeled in yellow.

Table S7, related to Figure5. Neutralization of N6 alanine variants against six VRC01-resistant viruses and two VRC01-sensitive viruses.

N6 Region	N6 Variant ID	Neutralization IC_{50}								Median IC_{50} (μg/ml)[a]	Fold change[b]	Breadth %
		VRC01-Resistant Viruses						VRC01-Sensitive Viruses				
		6540.v4.c1	T250-4	HO86.8	6631.V3.C10	DU422.01	X2088.c9	BG1168.01	CAAN.A2			
	WT	0.111	0.014	2.37	0.363	0.076	0.106	0.307	0.469	0.109		100
FRH1	T28A	0.042	0.018	25.9	0.259	>50	0.111	0.287	0.183	0.185	2	83
	T30A	0.050	0.014	5.16	0.217	0.027	0.074	0.237	0.180	0.062	1	100
CDRH1	I33A	22.3	0.188	>50	0.438	>50	0.130	0.319	0.278	11.37	105	67
	F35A	0.149	0.140	>50	0.229	0.210	0.130	0.192	0.326	0.180	2	83
FRH2	W47A	>50	>50	>50	34.2	5.84	34.4	0.709	0.662	42.20	389	50
	W50A	>50	48.1	>50	>50	0.073	>50	0.280	0.236	50.00	461	33
	K52A	>50	0.673	>50	0.845	0.480	0.183	0.416	0.239	0.759	7	67
	Q53A	0.048	0.011	1.16	0.357	2.85	0.111	0.305	0.340	0.234	2	100
	Y54A	1.02	0.055	>50	1.05	>50	0.224	0.459	0.356	1.035	10	67
	G55A	2.01	0.024	>50	0.465	0.130	0.142	0.384	0.338	0.304	3	83
	V57A	4.39	0.012	>50	0.311	1.53	0.163	0.287	0.285	0.921	8	83
CDRH2	N58A	>50	0.063	>50	8.34	0.071	0.183	0.234	0.268	4.262	39	67
	F59A	0.642	0.034	>50	0.888	>50	0.109	0.460	0.229	0.765	7	67
	G60A	0.069	0.017	>50	0.258	5.17	0.069	0.308	0.178	0.164	2	83
	G61A	0.034	0.010	5.85	0.215	10.1	0.075	0.213	0.207	0.145	1	100
	G62A	0.155	0.016	1.88	0.266	33.9	0.100	0.414	0.304	0.211	2	100
	R64A	>50	0.169	>50	7.20	1.44	0.112	0.974	0.293	4.320	40	67
	D65A	0.026	0.010	0.216	0.133	>50	0.067	0.132	0.145	0.100	1	83
	R71A	>50	31.6	>50	15.6	0.151	1.96	1.36	0.880	23.60	218	67
FRH3	V73A	0.391	0.008	4.03	0.149	0.070	0.067	0.191	0.185	0.110	1	100
	Y74A	4.33	0.023	>50	0.538	0.091	0.208	0.348	0.255	0.373	3	83
	G99A	0.012	0.009	0.370	0.203	0.090	0.066	0.214	0.151	0.078	1	100
CDRH3	D100A	4.09	0.007	>50	0.384	0.273	0.109	0.206	0.198	0.329	3	83
	S100AA	0.160	0.051	>50	0.198	3.38	0.106	0.273	0.269	0.179	2	83
	W100CA	>50	>50	>50	18.0	>50	>50	0.916	0.585	50.00	461	17
FRL1	Y1A	0.010	0.020	2.21	0.383	0.697	0.097	0.265	0.130	0.240	2	100
	I2A	0.018	0.022	>50	0.560	12.6	0.111	0.300	0.243	0.336	3	83
	Q27A	0.064	0.008	3.20	0.168	0.059	0.078	0.209	0.214	0.071	1	100
	G28A	0.018	0.013	>50	0.857	8.37	0.309	0.256	0.096	0.583	5	83
CDRL1	V29A	0.028	0.025	>50	0.449	1.65	0.083	0.375	0.146	0.266	2	83
	G30A	0.137	0.021	>50	0.656	0.646	0.165	0.413	0.286	0.406	4	83
	D32A	0.403	0.014	>50	0.665	4.39	0.155	0.303	0.245	0.534	5	83
	V90A	0.132	0.024	>50	0.538	2.29	0.125	0.343	0.212	0.335	3	83
CDRL3	L91A	>50	0.017	>50	14.2	0.161	8.78	0.340	0.304	11.49	106	67
	F97A	0.054	0.017	0.588	0.480	0.069	0.112	0.311	0.396	0.091	1	100

[a]Median IC_{50} is calculated based on VRC01-resistant viruses. In cases where neutralization IC_{50} was not achieved at the highest concentration of antibody, the highest concentration was used in calculation of the median.

[b] Fold change is defined as IC_{50} of antibody mutant/ IC_{50} of antibody WT. Regions that result in fold change values >100 are highlighted in red, values between 30-100 are highlighted in yellow. Values between 5-30 are highlighted in green.

Table S8, related to Figure 6. NGS statistics.

Chain	Time point	Input cells	Run	Raw pairs	Pair reads merged	VJ_ assigned	Functional	Unique reads	Percent of unique reads/ input cells (%)
Heavy	2012-12	310,000	1st	2585189	884323	815799	612690	19760	6.4
			2nd	4143998	2079434	1848789	1479846	22370	7.2
			3rd	4788972	2488448	2189633	1754484	22905	7.4
			Total	11518159	5452205	4854221	3847020	45222	14.6
	2014-05	80,000	1st	679180	208073	190233	141639	5803	7.3
			2nd	1276521	579269	510507	404666	7926	9.9
			3rd	1446569	688048	598996	480523	8059	10.0
			Total	3402270	1475390	1299736	1026828	13507	16.9
	2015-05	88,000	1st	528092	222157	211985	160498	5932	6.7
			2nd	1248166	772041	715578	577869	9162	10.4
			3rd	1431224	926487	853586	690293	9736	11.1
			Total	3207482	1920685	1781149	1428660	15220	17.3
Light	2012-12	310,000	1st	3162392	1723279	1690667	1503053	45761	14.8
			2nd	4438652	2769258	2685108	2434807	48173	15.5
			3rd	5032858	3180176	3071393	2775015	50592	16.3
			Total	12633902	7672713	7447168	6712875	71021	22.9
	2014-05	80,000	1st	982741	553790	543624	488933	14548	18.2
			2nd	1325501	838566	818524	748045	14979	18.7
			3rd	1534253	976084	948749	863378	15435	19.2
			Total	3842495	2368440	2310897	2100356	20339	25.4
	2015-05	88,000	1st	869934	631220	622927	562457	13906	15.8
			2nd	1232088	949867	931652	853715	14884	16.9
			3rd	1415300	1104776	1081712	988440	15622	17.8
			Total	3517322	2685863	2636291	2404612	21450	24.4

Supplementary Experimental Procedures

Donor Z258 information

Donor Z258 was selected for B-cell sorting and antibody generation because his serum neutralizing activity is among the most potent and broad in our cohort. The criteria for enrolment were as follows: having a detectable viral load, a stable CD4 T-cell count above 400 cells/μl, being diagnosed with HIV infection for at least 4 years, and off antiretroviral treatment for at least 5 years.

Memory B-cell staining, sorting and antibody cloning

As previously described (Huang et al., 2013), a total of 75,000 $CD19^{+}IgA^{-}IgD^{-}IgM^{-}$ memory B cells were sorted and re-suspended in medium with IL-2, IL-21 and irradiated 3T3-msCD40L feeder cells, and seeded into 384-well microtitre plates at a density of 4 cells per well. After 13 days of incubation, supernatants from each well were screened for neutralization activity using a high-throughput micro-neutralization assay against HIV-$1^{MN.3}$ and HIV-$1^{Bal.26}$. From the wells that scored positive in both the HIV-$1_{MN.3}$ and HIV-$1^{Bal.26}$ neutralization assay, the variable region of the heavy chain and the light chain of the immunoglobulin gene were amplified by RT–PCR and re-expressed as described previously (Georgiev et al., 2013; Tiller et al., 2008).

Generation of pseudoviruses

HIV-1 *env* pseudoviruses were generated by co-transfection of 293T cells with an *env*-deficient backbone (pSG3Δ*env*) and a second plasmid that expressed HIV-1 Env at a ratio of 2:1. 72h after transfection, supernatants containing pseudoviruses were harvested and frozen at −80°C until further use. JRCSF mutants were produced by altering the JRCSF *Env* plasmid with QuikChange Lightning site-directed mutagenesis kit according to the manufacturer's protocol (Agilent).

Neutralization assays

As described previously(Li et al., 2005), heat-inactivated patient serum or monoclonal antibody (mAb) was serially diluted five-fold with Dulbecco's modified Eagle medium–10% FCS (Gibco), and 10 μl of serum or mAb was incubated with 40 μl of pseudovirus in a 96-well plate at 37°C for 30 min. TZM-bl cells were then added and plates were incubated for 48h. Assays were then developed with a luciferase assay system (Promega, Finnboda Varvsväg, Sweden), and the relative light units (RLU) were read on a luminometer (Perkin Elmer).

Cross-competition ELISA

Cross-competition ELISA was performed following the method published previously (Wu et al., 2010). HIV_{YU2} gp120 at 2 μg/ml was coated on 96-well plates overnight at 4°C. Plates were blocked with B3T buffer (PBS, 3.3% FBS, 2% BSA, 0.07% Tween-20, 0.02% thimerosal, 150 mM NaCl, 50 mM Tris-HCl, and 1 mM EDTA) for 1 h at 37°C. 50 μl of serially diluted non-biotinylated competitor antibodies was added to the plate in B3T buffer, followed by addition of 50 μl of biotinylated antibody or CD4-Ig at a fixed concentration: 250 ng/ml of VRC01-biotin, 5 μg/ml of VRC23-biotin, 1 μg/ml of VRC-PG04-biotin or 150 ng/ml of CD4-Ig-biotin. Plates were incubated for 1h at 37°C. 1:200 dilution of HRP-conjugated streptavidin (BD) was added and incubated for 30 min at room temperature. Plates were washed between each step with

0.2% Tween-20 in PBS. Plates were developed using 3,3′,5,5′-tetramethylbenzidine (TMB)(Sigma -Aldrich) and read at 450 nm.

Binding assays

HIV^{BAL26} gp120 monomers, gp120 RSC3 and their CD4 knockout mutants gp120D368R and RSC3 Δ371I P363N at 2 μg/ml were coated on 96-well plates overnight at 4°C. Plates were blocked with BLOTTO buffer (PBS, 1% FBS, 5% non-fat milk) for 1 h at room temperature, followed by incubation with antibody serially diluted in disruption buffer (PBS, 5% FBS, 2% BSA, 1% Tween-20) for 1 h at room temperature. 1:10,000 dilution of horseradish peroxidase (HRP)-conjugated goat anti-human IgG antibody was added for 1h at room temperature. Plates were washed between each step with 0.2% Tween 20 in PBS. Plates were developed using TMB and read at 450 nm.

X-ray crystallography

The antigen binding fragment of N6 and deglycosylated HIV-1 core E gp120 were prepared as previously described (Zhou et al., 2010). The gp120-antibody complexes were formed by mixing deglycosylated gp120 with the antibody Fab in a 1:2 molar ratio. The complexes were purified by size exclusion chromatography (Hiload 26/60 Superdex S200 prep grade; GE Healthcare) with buffer containing 0.15 M NaCl and 5 mM HEPES (pH 7.5). Fractions with gp120-antibody complexes were concentrated to ~10 mg/ml and used for crystallization experiments. All gp120-Fab complexes were screened against 576 crystallization conditions using a Cartesian Honeybee crystallization robot. Initial crystals were grown by the vapor diffusion method in sitting drops at 20 °C by mixing 0.1 μl of protein with 0.1 μl of reservoir solution. Crystals were manually reproduced in hanging drops by mixing 0.50 μl of protein with 0.5 μl reservoir solution.

The 93TH057 Core E gp120-N6 complex was crystallized with a reservoir solution of 10 % w/v PEG 3350, 2 % (v/v) isopropanol, 0.1 M $CaCl_2$, 0.1 M HEPES, pH 7.5 and was flash frozen in liquid nitrogen with 30 %(v/v) ethylene glycol as a cryoprotectant. The DU172 CoreE gp120-N6 complex was crystallized with a reservoir solution of 7 % w/v PEG 4000, 4 % (v/v) isopropanol, 2 % (v/v) benzamidine, 0.1 M HEPES, pH 7.5 and was flash frozen in liquid nitrogen with 30 %(v/v) ethylene glycol as a cryoprotectant. The X2088 Core E gp120 was crystallized with a reservoir solution of 6% w/v PEG 3350, 20% MPD, 0.1 M imidazole pH 6.5 and 0.2M $(NH_4)_2SO_4$, and was flash frozen in liquid nitrogen with 15% 2R,3R-butanediol as a cryoprotectant.

Diffraction data for all crystals were collected with 1.0000Å x-ray wavelength at SER-CAT beamlines ID-22 (Advanced Photon Source, Argonne National Laboratory). Diffraction data were processed with the HKL2000 suite. For the N6-93TH057 crystal structure, molecular replacement solutions were obtained using PDB ID 3NGB as a search model. For the N6 structures in complex with DU172 and X2088, the solved N6-93TH057 complex was used as a molecular replacement model.

All structure was solved by molecular replacement with Phaser (McCoy et al., 2007). Iterative model building and refinement procedures were carried out using Coot (Emsley and Cowtan, 2004) and Phenix(Adams et al., 2010) (Supplemental Experimental Procedures and Table S4). Throughout the refinement processes, a cross validation (R_{free}) test set consisting of 5% of the data was used. Structure validations were performed periodically during the model building/refinement process with MolProbity. All figures containing representations of protein crystal structures were made with PyMOL. Interface between gp120 and antibody were analyzed with the PISA server.

Capture ELISA

The relative binding capacity of monomeric gp120 and N6 was determined by a gp120 capture enzyme-linked immunosorbent assay (ELISA) as previously described (Moore et al., 1995). 100 µl of anti-gp120 D7324 (Aalto Bioreagent, Dublin, Ireland) at 1 µg/ml in PBS was coated on 96-well plates overnight at 4°C. JRCSF pseudovirus stocks treated with Triton X-100 (0.5%) were added and incubated for 2 h at 37°C. Plates were blocked with B3T buffer for 1 h at 37°C, followed by incubation with antibody serially diluted in B3T buffer for 1 h at 37°C. 1:10,000 dilution of horseradish peroxidase (HRP)-conjugated goat anti-human IgG antibody (Jackson ImmunoResearch Laboratories) was added for 1 h at 37°C. Plates were washed between each step with 0.2% Tween-20 in PBS, developed using TMB and read at 450 nm.

Autoreactivity assays

Reactivity to HIV-1 negative human epithelial (HEp-2) cells was determined by indirect immunofluorescence on slides using FITC-conjugated goat anti-human IgG (Zeus Scientific)(Haynes et al., 2005). Slides were photographed on a Nikon Eclipse E800 microscope. Kodachrome slides were taken of each monoclonal antibody binding to HEp-2 cells at a 10-s exposure, and the slides scanned into digital format. The Luminex AtheNA Multi-Lyte ANA test (Wampole Laboratories) was used to test for monoclonal antibody reactivity to SSA/Ro, SS-B/La, Sm, ribonucleoprotein (RNP), Jo-1, double-stranded DNA, centromere B, and histone and was performed as per the manufacturer's specifications and as previously described(Haynes et al., 2005). Monoclonal antibody concentrations assayed were 50 µg/ml. 10 µl of each concentration was incubated with the Luminex fluorescent beads and the test performed per the manufacturer's specifications.

Protein array

Antibodies were screened for binding on protein microarrays (ProtoArray) (catalog no. PAH0525101; Invitrogen) precoated with >9,400 human proteins in duplicate. The binding patterns of human bNAbs were compared to the human myeloma protein 151K in lot-matched arrays. Array-bound anti-human IgG served as the loading control for the detection Ab, and array-bound human IgG served as the loading control for the secondary reagent.

Antibodies were screened for reactive Ags on protein microarrays following the manufacturer's instructions and as described previously (Yang et al., 2013). Briefly, the ProtoArray microarray (Invitrogen) was blocked and incubated on ice with 2 µg/ml of HIV-1 Ab or isotype control 151K for 90 min. Ab binding to array protein was detected with 1 µg/ml of Alexa Fluor 647-labeled anti-human IgG (Invitrogen) secondary Ab. The ProtoArray microarrays were scanned using a GenePix 4000B scanner (Molecular Devices) at a wavelength of 635 nm, with 10-µm resolution, using 100% power and 650 gain. Fluorescence intensities were quantified with GenePix Pro 5.0 program (Molecular Devices) using lot-specific protein location information provided by the microarray manufacturer.

Protoarray data analysis

The fluorescence intensity of HIV-1 Abs binding to each protein on the microarray was graphed against that of control Ab, 151K. The distance of each data point to the reference line, y = x (i.e., R = 1 [the diagonal line]), was determined using the distance formula: $d = (x - y)/\sqrt{2}$ on the log scale. This formula was derived using triangulation of distances to the reference line. Comparisons of averaged binding to array proteins were

similar for 151K, palivizumab, and infliximab, indicating that these three IgG1(κ) Abs had similar levels of unspecific binding; in consequence (see Results), polyreactivity was defined as a 2-fold increase in averaged binding compared to the binding of 151K. Mathematically, the polyreactivity threshold (PT) equals the distance of x = 2y to the reference line (y = x): PT = (log10 x − log10 y)/$\sqrt{2}$ = log10 (x/y)/$\sqrt{2}$ = log10 2/$\sqrt{2}$ = 0.21.

To assess HIV-1 Ab polyreactivity, the distance of each data point to a reference line, y = x, was determined and graphed as a frequency histogram, with a mean fluorescence intensity (MFI) bin size of 0.02 (resolution threshold of GenePix 4000B scanner). The Gaussian mean of array protein distances from the y = x reference line is the polyreactivity index (PI), and determined by GraphPad software. When the PI of an HIV-1 Ab is greater than the PT (>0.21), the mean of the MFI for all array proteins was >2-fold over the control mean, defining the test Ab as polyreactive. Abs that were not polyreactive (PI ≤ 0.21) were defined as autoreactive if they recognized specific human proteins ≥500-fold more avidly than 151K.

Viral RNA extraction and cDNA synthesis

As described previously (Wu et al., 2012), viral RNA of patient Z258 was extracted from 280 µl of serum sample from two different time points using the QIAamp viral RNA mini kit (Qiagen) and eluted in 50 µl of elution buffer. The first-strand cDNA synthesis was carried out using the SuperScript III reverse transcriptase (Invitrogen Life Technologies). The final 100-ul reaction volume was composed of 50 µl viral RNA, 5 µl of a deoxynucleoside triphosphate (dNTP) mixture (each at 10 mM), 1.25 µl antisense primer envB3out (5′-TTGCTACTTGTGATTGCTCCATGT-3′) at 20 µM, 20 µl 5× first-strand buffer, 5 µl dithiothreitol at 100 mM, 5 µl RNaseOUT and 5 µl SuperScript III reverse transcriptase. RNA, primers, and dNTPs were heated at 65°C for 5 min and then chilled on ice for 1 min, and then the entire reaction mixture was incubated at 50°C for 60 min, followed by 55°C for an additional 60 min. Finally, the reaction was heat inactivated at 70°C for 15 min and then treated with 1 µl RNase H at 37°C for 20 min. The resulting cDNA was used immediately for PCR or frozen at 80°C to await further analysis.

SGA

The nested PCR of HIV-1 *env* SGA was described previously (Wu et al., 2012). Briefly, the cDNA was serially diluted and distributed in replicates of 12 PCR reactions in ThermoGrid 96-well plates (Denville Scientific) to identify a dilution where PCR-positive wells constituted about 30% of the total number of reactions. At this dilution, most of the positive wells contain amplicons derived from a single cDNA molecule. Additional PCR amplifications were performed using this dilution in full 96-well plates. PCR amplification was carried out using the Platinum *Taq* High Fidelity PCR system (Invitrogen Life Technologies). The final 20-µl reaction volume was composed of 2 µl 10× buffer, 0.8 µl $MgSO_4$, 0.4 µl dNTP mixture (each at 10 mM), 0.2 µl each primer at 20 µM, 0.1 µl Platinum *Taq* High Fidelity polymerase, and 1 µl template DNA. The primers for the first-round PCR were envB5out (5′-TAGAGCCCTGGAAGCATCCAGGAAG-3′) and envB3out (5′-TTGCTACTTGTGATTGCTCCATGT-3′). The primers for the second-round PCR were envB5in (5′-CACCTTAGGCATCTCCTATGGCAGGAAGAAG-3′) and envB3in (5′-GTCTCGAGATACTGCTCCCACCC-3′). The cycler parameters were 94°C for 2 min, followed by 35 cycles of 94°C for 15 s, 55°C for 30 s, and 68°C for 4 min and by a final extension of 68°C for 10 min. The product of the first-round PCR (1 µl) was subsequently used as the template in the second-round PCR under the same conditions but with a total of 45 cycles. The amplicons were inspected on a precast 1% agarose gel (Embi Tec). All PCR procedures were carried out in a designated PCR clean hood using procedural

safeguards against sample contamination.

DNA sequencing

Amplicons were directly sequenced by BigDye Terminator chemistry by ACGT, Inc. (Wheeling, IL). Both DNA strands were sequenced using partially overlapping fragments. Individual sequence fragments for each amplicon were assembled and edited using Sequencher 5.0 (Gene Codes, Ann Arbor, MI). All chromatograms were inspected for sites of mixed bases (double peaks), which would be evidence of priming from more than one template or the introduction of PCR error in early cycles. Any sequence with evidence of double peaks was excluded from further analysis.

Cloning of donor Z258 HIV-1 *env* genes

Representative *env* sequences from donor Z258 were selected for cloning. The second-round *env* PCR products containing full-length *rev* and *env* genes were amplified using Herculase II Fusion DNA Polymerase (Agilent Technologies), primers HIV RevS (CACCATGGCAGGAAGAAG) and envB3in (5′-GTCTCGAGATACTGCTCCCACCC-3′) with the same conditions of the second-round PCR as described above. PCR amplicons were gel-purified and ligated into the expression vector pcDNA3.1D (Invitrogen Life Technologies) under the control of the T7 promoter. Plasmids were transfected into TOP10 Chemically Competent *E. coli* (Invitrogen Life Technologies), each expression plasmid was isolated as a maxiprep (Qiagen), and its sequence was verified. Of a total of eleven *env* sequences cloned from donor Z258, eleven (100%) were functional in mediating virus entry.

Next Generation Sequencing (NGS) of the PBMC memory B cells

Sequencing of expressed Ig genes was performed using a previously described method (Gros et al., 2014) but with changes to 3' PCR primer sequences. B cell receptor sequences were analyzed using a 5' RACE technique that permits an unbiased examination of the B cell repertoire (He et al., 2014). The product was sequenced using Illumina MiSeq, with an average sequencing depth of ~40x (Table S8). Briefly, sorted cells were lysed and total RNA was extracted using RNAzol RT (Molecular Research Center Inc., Cincinnati, OH). cDNA was synthesized using a modified version of the SMARTer cDNA Synthesis kit (Clontech, Mountain View, CA). IGHG and IGLK sequences were then amplified using the SMARTer 5' primer and Ig-specific 3' primers: IgG (5'-GCCAGGGGGAAGACCGATGGGCCCTTGGTGGA-3') or IgK (5'-GCGGGAAGATGAAGACAGATGGTGCAGCCACAG-3'). The amplicons were amplified further to incorporate the Illumina flow cell binding sequences, Illumina read 1 sequences, and unique identifiers. These Illumina-ready libraries were sequenced by paired end Illumina 2x300 reads to obtain full-length VDJ sequences.

NGS data processing

The 2x300 raw reads were assembled to single end transcripts using USEARCH (Edgar and Flyvbjerg, 2015). Transcripts containing more than 10 sequencing errors estimated using Usearch were excluded. Then the transcripts were processed using our in-house implemented bioinformatics pipeline (Wu et al., 2015). Briefly, transcripts shorter than 300 nucleotides were removed. BLAST (http://www.ncbi.nlm.nih.gov/blast/) was used to assign germline V, D, and J genes to each transcript with customized parameters. Sequences other than the V(D)J region of a transcript were removed and transcripts containing frame-shift or stop codon

were excluded. The sequence identities of each transcript to germline V gene, N6, F8, N17, and VRC27 were calculated using ClustalO (Sievers et al., 2011) and were shown in 2D heatmaps plotted using ggplot2 in R.

Identification of N6 lineage related transcripts from NGS

To find lineage related heavy chain transcripts, we used ClustalO (Sievers et al., 2011) to calculate the sequence identity of CDR3 of each transcript in each dataset to that of N6, F8, N17, and VRC27. Transcripts with germline V gene assignment to IGHV1-2, sequence identity of CDR3 higher than 60% to N6, F8, N17, or VRC27, and the length of CDR3 in the range of 10-20 amino acids, were sieved for further analyses. To remove PCR duplicates and transcripts containing sequencing errors, two steps of clustering were performed using USEARCH. The transcripts were firstly clustered at 100% sequence identity and the transcripts were ranked by sequence coverage. Then the transcripts with high coverage were used as seeds or centers for the second step of clustering at 97% sequence identity. One representative sequence was selected from each cluster containing more than one transcripts and a curated unique dataset was then generated for each time point. We then manually removed non-related transcripts from the curated dataset.

To find lineage related light chain transcripts, we first identified transcripts containing the CDR3 signatures (X-X-[AFILMYWV]-[EQ]-X,) of the VRC01 class (Zhou et al., 2013). Two steps of clustering were then performed to remove PCR duplicates and transcripts containing sequencing errors (See heavy chain data processing). Finally, a curated unique light chain dataset was generated for each time point and non-related transcripts were manually removed.

Phylogenetic analyses and inference of intermediates

The lineage related transcripts of heavy and light chains were aligned separately using Muscle and manually adjusted. Maximum likelihood phylogenetic trees for heavy and light chains were constructed using MEGA6 (Tamura et al., 2013). The GTR+G+I substitution model, selected using MEGA6 as the best overall model for fitting to the sequence datasets (Tamura et al., 2013), was used to estimate genetic distance. Five categories were used when modelling rate heterogeneity by Γ distribution. The phylogenetic trees of heavy and light chains were rooted using IGHV1-2*02 and IGKV1-33*01 respectively. The rooted phylogenetic trees and aligned sequences were input into MEGA6 to infer intermediates using the maximum likelihood method (Tamura et al., 2013).

Supplemental References

Adams, P.D., Afonine, P.V., Bunkoczi, G., Chen, V.B., Davis, I.W., Echols, N., Headd, J.J., Hung, L.W., Kapral, G.J., Grosse-Kunstleve, R.W.*, et al.* (2010). PHENIX: a comprehensive Python-based system for macromolecular structure solution. Acta Crystallogr D Biol Crystallogr *66*, 213-221.

Edgar, R.C., and Flyvbjerg, H. (2015). Error filtering, pair assembly and error correction for next-generation sequencing reads. Bioinformatics *31*, 3476-3482.

Emsley, P., and Cowtan, K. (2004). Coot: model-building tools for molecular graphics. Acta Crystallogr D Biol Crystallogr *60*, 2126-2132.

Gros, A., Robbins, P.F., Yao, X., Li, Y.F., Turcotte, S., Tran, E., Wunderlich, J.R., Mixon, A., Farid, S., Dudley, M.E.*, et al.* (2014). PD-1 identifies the patient-specific CD8(+) tumor-reactive repertoire infiltrating human tumors. The Journal of clinical investigation *124*, 2246-2259.

Haynes, B.F., Fleming, J., St Clair, E.W., Katinger, H., Stiegler, G., Kunert, R., Robinson, J., Scearce, R.M., Plonk, K., Staats, H.F.*, et al.* (2005). Cardiolipin polyspecific autoreactivity in two broadly neutralizing HIV-1 antibodies. Science *308*, 1906-1908.

He, L., Sok, D., Azadnia, P., Hsueh, J., Landais, E., Simek, M., Koff, W.C., Poignard, P., Burton, D.R., and Zhu, J. (2014). Toward a more accurate view of human B-cell repertoire by next-generation sequencing, unbiased repertoire capture and single-molecule barcoding. Sci Rep *4*, 6778.

Krissinel, E., and Henrick, K. (2007). Inference of macromolecular assemblies from crystalline state. J Mol Biol *372*, 774-797.

McCoy, A.J., Grosse-Kunstleve, R.W., Adams, P.D., Winn, M.D., Storoni, L.C., and Read, R.J. (2007). Phaser crystallographic software. J Appl Crystallogr *40*, 658-674.

Moore, J.P., Cao, Y., Qing, L., Sattentau, Q.J., Pyati, J., Koduri, R., Robinson, J., Barbas, C.F., 3rd, Burton, D.R., and Ho, D.D. (1995). Primary isolates of human immunodeficiency virus type 1 are relatively resistant to neutralization by monoclonal antibodies to gp120, and their neutralization is not predicted by studies with monomeric gp120. J Virol *69*, 101-109.

Sievers, F., Wilm, A., Dineen, D., Gibson, T.J., Karplus, K., Li, W.Z., Lopez, R., McWilliam, H., Remmert, M., Soding, J.*, et al.* (2011). Fast, scalable generation of high-quality protein multiple sequence alignments using Clustal Omega. Molecular systems biology *7*.

Tamura, K., Stecher, G., Peterson, D., Filipski, A., and Kumar, S. (2013). MEGA6: Molecular Evolutionary Genetics Analysis version 6.0. Mol Biol Evol *30*, 2725-2729.

Tiller, T., Meffre, E., Yurasov, S., Tsuiji, M., Nussenzweig, M.C., and Wardemann, H. (2008). Efficient generation of monoclonal antibodies from single human B cells by single cell RT-PCR and expression vector cloning. Journal of immunological methods *329*, 112-124.

Wu, X., Yang, Z.Y., Li, Y., Hogerkorp, C.M., Schief, W.R., Seaman, M.S., Zhou, T., Schmidt, S.D., Wu, L.,

Xu, L.*, et al.* (2010). Rational design of envelope identifies broadly neutralizing human monoclonal antibodies to HIV-1. Science *329*, 856-861.

Yang, G., Holl, T.M., Liu, Y., Li, Y., Lu, X., Nicely, N.I., Kepler, T.B., Alam, S.M., Liao, H.X., Cain, D.W.*, et al.* (2013). Identification of autoantigens recognized by the 2F5 and 4E10 broadly neutralizing HIV-1 antibodies. J Exp Med *210*, 241-256.

Zhou, T., Georgiev, I., Wu, X., Yang, Z.Y., Dai, K., Finzi, A., Kwon, Y.D., Scheid, J.F., Shi, W., Xu, L.*, et al.* (2010). Structural basis for broad and potent neutralization of HIV-1 by antibody VRC01. Science *329*, 811-817.